Novel isoniazid embedded triazole derivatives: Synthesis, antitubercular and antimicrobial activity evaluation

Pravin S. Patil[a], Sanghratna L. Kasare[a], Nitin B. Haval[a], Vijay M. Khedkar[b], Prashant P. Dixit[c], Estharla Madhu Rekha[d], Dharmarajan Sriram[d], Kishan P. Haval[a],*

[a] Department of Chemistry, Dr. Babasaheb Ambedkar Marathwada University SubCampus, Osmanabad 413501, MS, India
[b] Department of Pharmaceutical Chemistry, School of Pharmacy, Vishwakarma University, Pune 411048, MS, India
[c] Department of Microbiology, Dr. Babasaheb Ambedkar Marathwada University SubCampus, Osmanabad 413501, MS, India
[d] Department of Pharmacy, Birla Institute of Technology and Science-Pilani, Hyderabad Campus, Jawahar Nagar, Shameerpet Mandal, R. R. District, Hyderabad 500078, India

ABSTRACT

In the present study, a series of new isoniazid embedded triazole derivatives have been synthesized. These compounds were evaluated for their *in vitro* antitubercular and antimicrobial activities. Among the screened compounds, six have exhibited potent antitubercular activity against *Mycobacterium tuberculosis* H37Rv strain with MIC value 0.78 µg/mL, whereas, three compounds have displayed activity with MIC value ranging from 1.56 to 3.125 µg/mL. The cytotoxicity of the active compounds was studied against RAW 264.7 cell line by MTT assay and no toxicity was observed even at 25 µg/mL concentration. The five compounds have displayed good antimicrobial activities. Molecular docking have been performed against mycobacterial InhA enzyme to gain an insight into the plausible mechanism of action which could pave the way for our endeavor to identify potent antitubercular candidates. We believe that further optimization of these molecules may lead to potent antitubercular agents.

Tuberculosis (TB) is the leading cause of death from a single infectious agent (ranking above HIV/AIDS). It is a chronic disease that gets transmitted through air and caused by the bacillus *Mycobacterium tuberculosis*. It typically affects the lungs (pulmonary TB) but can also affect other sites (extrapulmonary TB).[1] As per Global Tuberculosis Report-2019, tuberculosis (TB) is a communicable disease and one of the top ten causes of death worldwide.[2] The current efforts in the drug development process are insufficient to completely eradicate the TB epidemic.[3] There are two main health concerns around the tuberculosis: drug-resistant tuberculosis and co-infection with HIV. It is observed that interest in tuberculosis research is rising, and the control of its spread has become one of the main health priorities in the world, with the United States, the United Kingdom, and India, leading the research in this area.[4] As constrained treatment options for multi-drug resistant (MDR-TB) and extensively drug resistant (XDR-TB) are available, TB researchers have the challenge of synthesizing new anti-TB drugs with novel modes of action.[5,6]

Isoniazid (**INH**) has been used as first-line anti-TB drug combined with Rifampicin (**RIF**), Ethambutol (**EMB**) and Pyrazinamide (**PZA**) to treat TB infection for more than 60 years, and it still remains one of the most effective anti-TB drugs. Its mechanism of action includes multiple effects on lipids, glycolysis, biomembranes, proteins and nucleic acid synthesis.[7] Unfortunately, it has several adverse effects particularly, psychiatric, hepatitis, peripheral neuropathy, GI Intolerance, allergic reactions and drug interactions.[8] The bacterial strains resistant to isoniazid are becoming common which mainly due to the long-term widely use even abuse, so there is an urgent need to develop novel isoniazid derivatives.[9]

To overcome the drug resistance and adverse effects, combination of isoniazid with other active moiety is frequently applied. Numerous efforts have been undertaken to develop isoniazid hybrids as new anti-TB agents (Fig. 1).[10–15] 1,2,3-Triazole derivatives inhibit the growth of bacteria by blocking lipid biosynthesis and/or additional mechanisms which is one of the most attractive strategies for developing effective anti-TB agents (development of cell wall biosynthesis inhibitors). Both isoniazid and triazole act by similar mechanism, i.e. inhibition of cell wall synthesis and both are very potent anti-TB agents, thus these two entities conjugated covalently into one single molecule may offer a new lead with potent anti-tubercular activity.[16–21] Recently, we have reported phthalimide bearing 1,2,3-triazole derivatives possessing

(a) Representative isoniazid and 1,2,3-triazole analogues having antitubercular activity

(A) LL-3858
(Lupin Ltd, MIC: 0.25 µg/mL)[10]

(B, MIC: 0.62 to 2.5 µg/mL)[11]

(C, MIC_{99}: 0.39 to 3.125 µM)[12]

(D, MIC_{99}: 0.195 to 0.39 µM)[13]

(E, MIC: 0.23 to 1.45 µM)[14]

(F, MIC_{90}: 0.03 to 1.6 µM)[15]
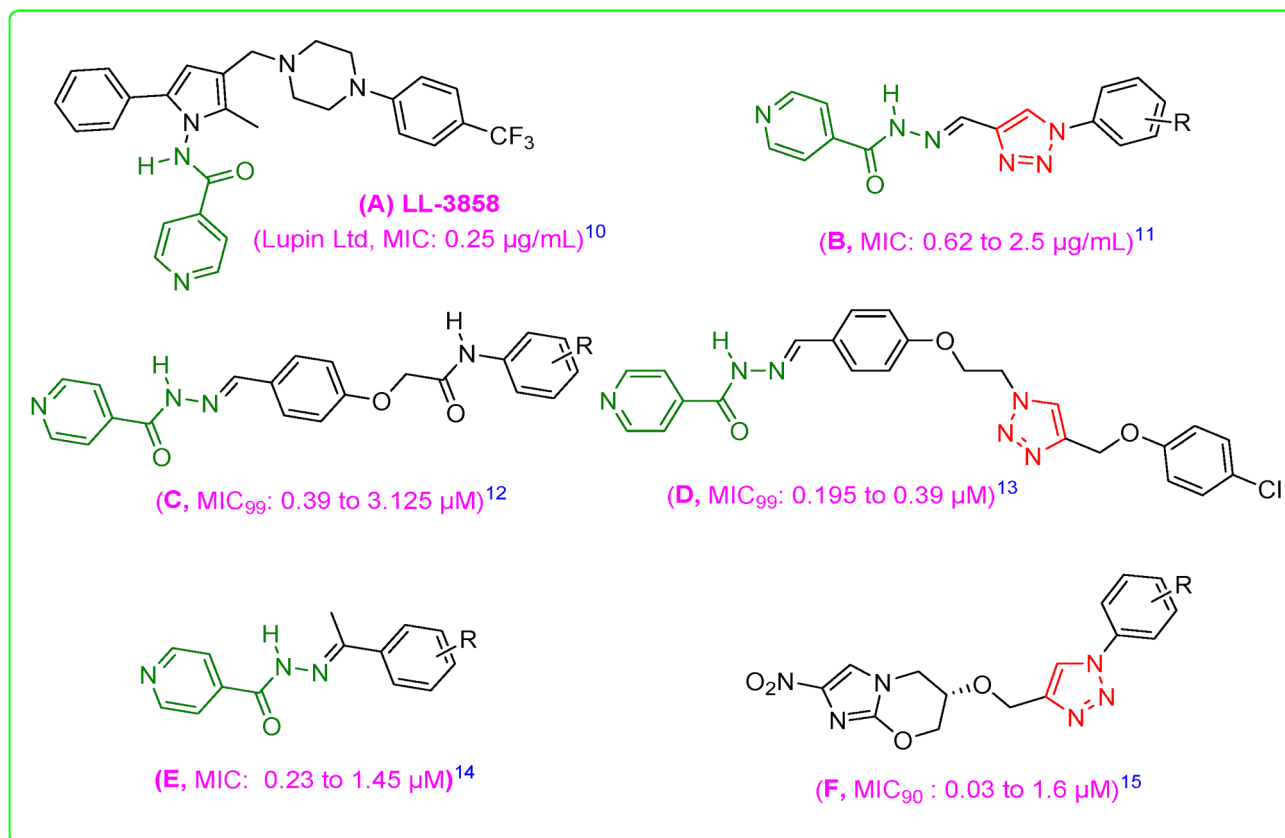
(b) Our approach: Isoniazid embedded triazole derivatives as antitubercular agents

INH Active anti-TB pharmcophore

Essential for activity

Lipophilic control
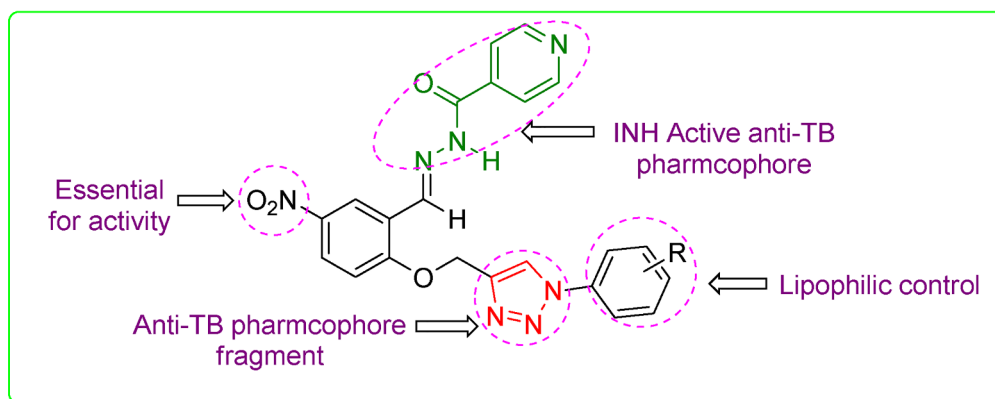
Anti-TB pharmcophore fragment

Fig. 1. (a) Representative isoniazid and 1,2,3-triazole analogues having antitubercular activity; (b) Our approach of isoniazid embedded triazole derivatives as antitubercular agents.

antitubercular activity.[22] Encouraged by the previous studies[23–28] and in continuation of our efforts towards the synthesis of new anti-tuberculosis agents, herein, we designed and synthesized a series of novel isoniazid embedded 1,4-disubstituted 1,2,3-triazole analogues starting from 5-nitrosalicylaldehyde.

For the synthesis of the title compounds, firstly 2-hydroxy-5-nitrobenzaldehyde (**1**) was treated with propargyl bromide in presence of K_2CO_3 in DMF at room temperature to obtain aldehyde (**2**).[29,42] The condensation of aldehyde (**2**) and isonicotinohydrazide was carried out in diisopropylethylammonium acetate (DIPEAc) to obtain the alkyne (**3**) (Scheme 1).[30,31,43] The click reaction of alkyne (**3**) and substituted azidobenzenes (**4a-p**) in presence of CuSO$_4$·5H$_2$O and sodium ascorbate

was performed to furnish corresponding triazole derivatives (**5a-p**) in good yields[44] as depicted in Scheme 2.

The newly synthesized compounds were characterized by their ^{1}H NMR, ^{13}CNMR and HRMS spectral data analysis. In ^{1}H NMR spectrum of compound **5o**, two singlets at δ 2.33 and 5.45 ppm are observed due to the –CH$_3$ attached to aromatic ring and –O-CH$_2$ attached to triazolyl ring, respectively. The characteristic peak at δ 12.02 is due to amide N−H. The two characteristics peaks in ^{13}CNMR spectrum of compound **5o** at δ 18.67 and 62.75 ppm confirms the presence of –CH$_3$ and –OCH$_2$ carbons, respectively. The HRMS spectrum further strengthen the structure assigned to compound **5o**, as it displays [M + H]$^+$ ion peak at m/z 503.1427 for the molecular formula $C_{23}H_{18}N_8O_6$.
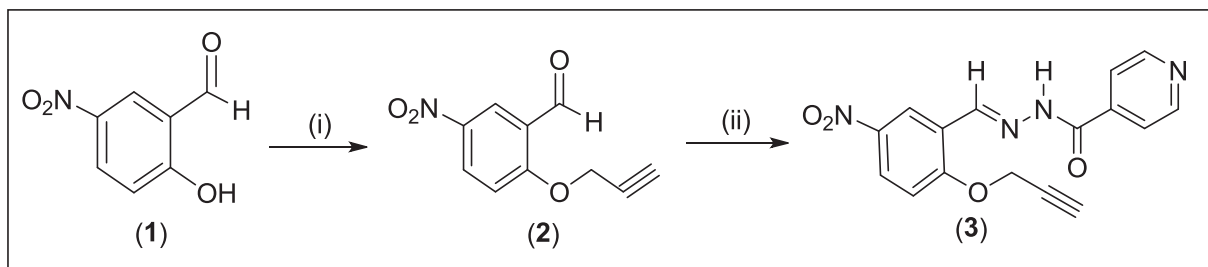
Scheme 1. *Reaction conditions*: (i) Propargyl bromide, K$_2$CO$_3$, DMF, rt, 6 h (90%); (ii) Isonicotinohydrazide, DIPEAc, rt, 1 h (92%).
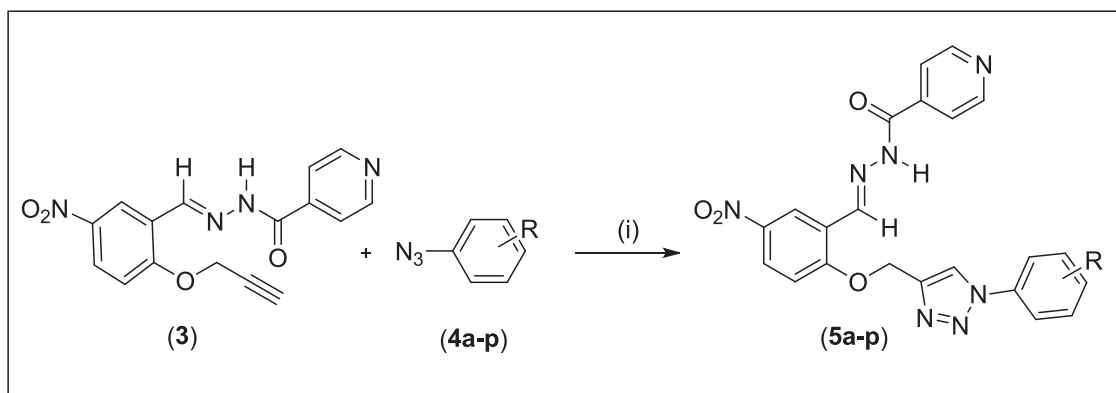
Scheme 2. *Reaction conditions*: (i) CuSO4, Sodium ascorbate, DMF, rt (80–92%).

The antitubercular screening was performed by preparing inoculum from fresh LJ medium re-suspended in 7H9-S medium (7H9 broth, 0.1% casitone, 0.5% glycerol, supplemented oleic acid, albumin, dextrose, and catalase [OADC]), adjusted to OD$_{590}$ 1.0, and diluted 1:20; 100 μL was used as inoculum. Each drug stock solution was thawed and diluted in 7H9-S at four-fold the final highest concentration tested. The serial two-fold dilutions of each drug were prepared directly in a sterile 96-well microtiter plate using 100 μL 7H9-S. A growth control containing no antibiotic and a sterile control were also prepared on each plate. Sterile water was added to all perimeter wells to avoid evaporation during the incubation. The plate was covered, sealed in plastic bags and incubated at 37 °C in normal atmosphere. After 7 days incubation, 30 μL of alamar blue solution was added to each well, and the plate was re-incubated overnight. A change in colour from blue (oxidised state) to pink (reduced) indicated the growth of bacteria, and the MIC was defined as the lowest concentration of drug that prevented this change in colour.[32,33] The compounds **5b**, **5d**, **5i**, **5 m**, **5o** and **5p** have shown excellent antitubercular activity with MIC value 0.78 μg/mL. While, compounds **5f**, **5j** and **5n** have displayed noticeable antitubercular activity with MIC value 1.56, 1.56 and 3.125 μg/mL, respectively (Table 1).
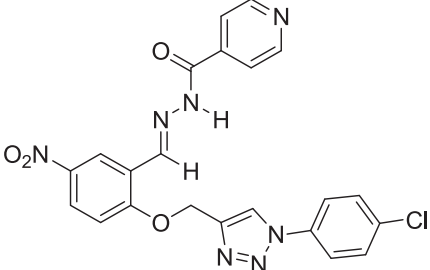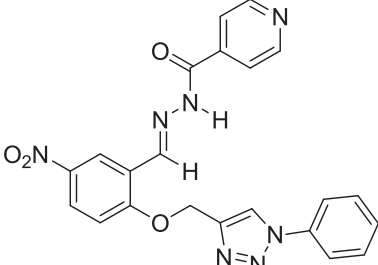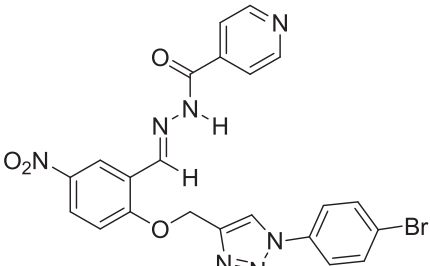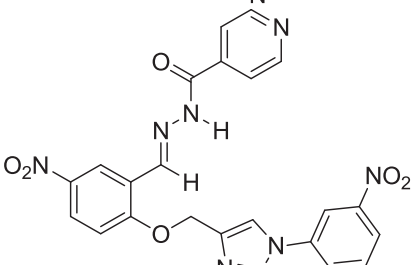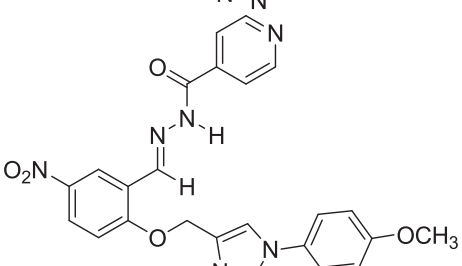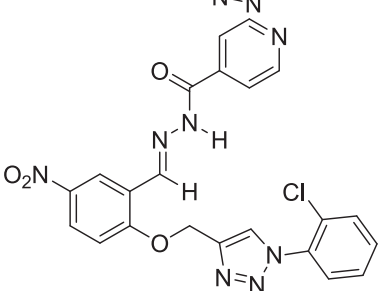
The *in vitro* cytotoxicity of the antitubercular active analogues with lower MIC value were assessed by 3-(4,5-dimethylthiazol-2-yl)-2,5-diphenyltetrazolium bromide (MTT) assay against growth inhibition of RAW 264.7 cells at 25 μg/mL concentration.[34] The cell lines were maintained at 37 °C in a humidified 5% CO$_2$ incubator (Thermo scientific). Detached the adhered cells and followed by centrifugation to get cell pellet. Fresh media was added to the pellet to make a cell count using haemocytometer and plate 100 μL of media with cells ranging from 5000–6000 per well in a 96-well plate. The plate was incubated overnight in CO$_2$ incubator for the cells to adhere and regain its shape. After 24 h, cells were treated with the test compounds at 25 μg/mL diluted using the media to deduce the percentage inhibition on normal cells. The cells were incubated for 48 h to assay the effect of the test compounds on different cell lines. Zero hour reading was noted down

with untreated cells and also control with 1% DMSO to subtract further from the 48 h reading. After 48 h incubation, cells were treated by MTT (4, 5-dimethylthiazol-2-yl)- 2, 5-diphenyltetrazolium bromide) dissolved in PBS (5 mg/ml) and incubated for 3–4 h at 37 °C. The formazan crystals thus formed were dissolved in 100 μL of DMSO and the viability was measured at 540 nm on a multimode reader (Spectra max). The values were further calculated for percentage inhibition, which in turn helps us to know the cytotoxicity of the test compounds. The results obtained are summarized in Table 1.

Newly synthesized isoniazid embedded triazole derivatives (**5a-p**) were evaluated for their *in vitro* antimicrobial activities against both Gram positive and negative bacteria by agar well diffusion assay.[35] Tetracycline and Fluconazole were used as reference standard for antibacterial and antifungal activities, respectively. The antibacterial pathogens DMSO was used as negative control. The compounds were dissolved in DMSO and concentration used for this assay was 1 mg/mL. Inoculums of each bacterial and fungal pathogen was developed by inoculating pathogens in nutrient broth and keeping them for 24 h at 37 °C. The bacterial suspension was diluted to adjust the turbidity to the 0.5 McFarland standards by using sterile saline. 200 μL diluted suspension of each pathogen was inoculated on sterile Mueller Hinton agar plates. Wells were prepared in agar and wells were filled with 100 μL of the samples. Incubation of all experimental Petri plates was allowed at 37 °C for 24 h. After incubation, the plates were keenly observed and results were recorded. Zones were measured and recorded by using scale in millimeter (mm). The compounds **5e**, **5f**, **5g**, **5h** and **5j** have exhibited good antimicrobial activities against both antibacterial and antifungal pathogens. The presence of –OCH$_3$ and –Cl substituents on these derivatives have played vital role for their activities. The compound **5i**, **5k** and **5l** have displayed moderate antimicrobial activities (Table 2).
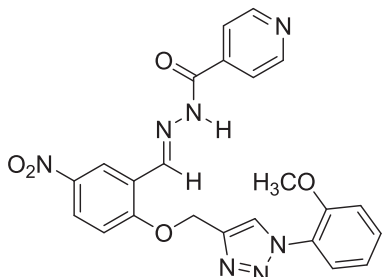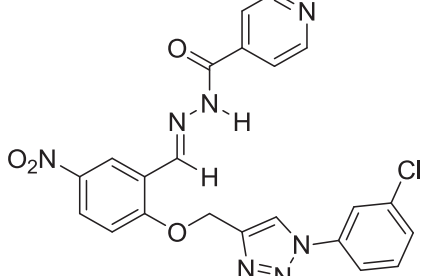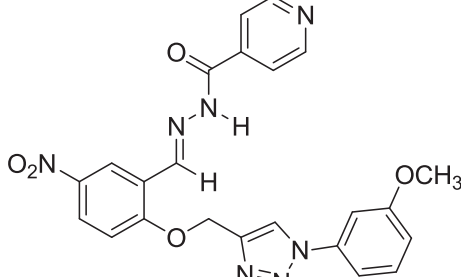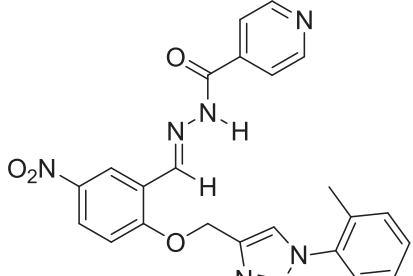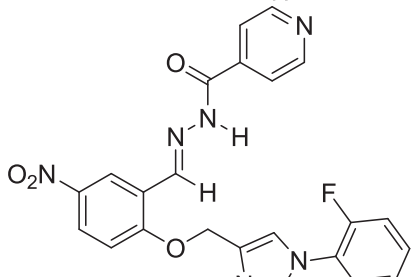
The MIC values were determined for the compounds having good antimicrobial activities and performed by following the method and guidelines of Clinical and Laboratory Standard Institute (CLSI). The results are summarized in Table 3 and expressed in μg/mL.

Table 1
Antimycobacterial activity of isoniazid embedded triazole derivatives (**5a-p**).

Entry	Triazole derivatives	Yield (%)	MIC against Mtb H37Rv strain (μg/mL)	% Inhibition Cytotoxicity at 25 μg/mL
5a		83	25	NA
5b		85	0.78	25.69
5c		82	12.5	19.04
5d		92	0.78	22.71
5e		84	> 25	NA
5f		82	1.56	24.18

(continued on next page)

Table 1 (*continued*)

Entry	Triazole derivatives	Yield (%)	MIC against Mtb H37Rv strain (µg/mL)	% Inhibition Cytotoxicity at 25 µg/mL
5g		86	> 25	NA
5h		84	12.5	20.12
5i		81	0.78	23.86
5j		83	1.56	24.16
5k		82	12.5	19.27

(*continued on next page*)

Table 1 (*continued*)

Entry	Triazole derivatives	Yield (%)	MIC against Mtb H37Rv strain (µg/mL)	% Inhibition Cytotoxicity at 25 µg/mL
5l		86	12.5	23.18
5m		80	0.78	27.72
5n		82	3.125	17.65
5o		90	0.78	23.88
5p		84	0.78	26.95
Isoniazid			0.1	
Rifampicin			0.2	
Ciprofloxacin			1.56	
Ethambutol			3.125	

Table 2
Antimicrobial activity of isoniazid embedded triazole derivatives (**5a-p**).

Entry	Pathogens										
	Antibacterial									Antifungal	
	S. aureus	*B. cerus*	*B. subtilis*	*E. aerogenes*	*E. coli*	*S. typhi*	*P. aeruginosa*	*S. boydii*	*S. abony*	*A. niger*	*S. cerevisiae*
5a	–	–	–	–	–	13	15	–	–	16	10
5b	–	–	–	14	12	–	13	–	–	–	10
5c	–	–	–	12	–	10	–	–	–	–	12
5d	–	–	–	–	–	–	–	–	–	–	–
5e	10	12	06	14	12	12	12	14	13	11	121
5f	12	11	09	10	12	10	–	07	–	10	12
5g	12	12	12	12	11	11	08	13	08	10	10
5h	15	10	11	13	10	10	08	12	10	09	10
5i	–	–	12	06	09	12	10	–	08	13	–
5j	13	12	11	10	–	11	10	14	12	09	12
5k	–	–	11	10	–	10	13	–	–	–	–
5l	13	13	10	08	–	10	12	–	–	08	–
5m	–	–	–	–	–	10	–	–	–	–	–
5n	–	–	–	–	–	11	–	–	–	–	–
5o	–	–	–	–	12	–	09	–	–	13	–
5p	–	–	–	–	10	–	10	–	–	10	–
Tetracycline	22	32	18	24	29	28	28	29	27	NA	NA
Fluconazole	NA	NA	NA	NA	NA	NA	NA	NA	NA	30	30

(–): Not active; NA: Not applicable; Diameter of zone of inhibition is given in millimeter (mm).

Table 3
MIC values of most potent isoniazid embedded triazole derivatives.

Pathogens	**5e**	**5f**	**5g**	**5 h**	**5j**	**Tetracycline**
S. typhi ATCC9207	340	170	230	140	270	20
S. aureus ATCC 6538	180	200	450	220	310	20
E. aerogenes ATCC13048	150	130	370	260	190	15

The significant anti-tubercular activities exhibited by isoniazid embedded triazole derivatives motivated us to elucidate the plausible target and mechanism of their antimycobacterial action. Molecular docking has emerged has a reliable tool complementary to the *in vivo* and *in vitro* biological study to identify the potential biological target and gain an insight into the ligand–receptor interactions for the bioactive molecules, especially in the absence of available resources to perform enzyme-based assays.[36,37] With this objective molecular docking study was carried out for these bioactive molecules against a crucial mycobacterial target enoyl ACP reductase (InhA) using the *Glide* (Grid-Based Ligand Docking With Energetics) program of the Schrödinger molecular modeling suite (Schrödinger, LLC, New York, NY, 2018).[38–41]

Molecular docking study revealed that all the bioactive isoniazid embedded triazole derivatives (**5b**, **5d**, **5f**, **5i**, **5j**, **5m**, **5n**, **5o** and **5p**) could recognize the binding site of InhA and got deeply embedded in it engaging in a network of bonded and non-bonded interactions. They have produced an average docking score (Glide Score) of −8.031 with an average binding energy (Glide energy) of −50.051 kcal/mol signifying a promising binding affinity towards the target. Furthermore, to gain a more detailed insight into the most significant interactions guiding the ligand-receptor binding, a per-residue interaction analysis was performed between these molecules and the active site residues (Table 4).

The lowest energy docked conformation of **5i** showed that the compound could snugly fit into the active site of mycobacterial enoyl ACP reductase (InhA) with an excellent binding affinity (Glide score of −8.395 and Glide binding energy −52.373 kcal/mol) at the co-ordinates close to the native ligand engaging in a series of steric and electrostatic interactions (Fig. 2).

The per-residue interaction analysis showed that the enzyme-inhibitor complex is stabilized by a network of favorable van der Waals interactions (steric) observed with active site residues wherein the 1-(2-methoxy phenyl)-1*H*-1,2,3-triazol-4-yl component interacted closely with Leu218 (−2.599 kcal/mol), Leu217 (−2.576 kcal/mol), Ile215 (−3.547 kcal/mol), Gln214 (−2.823 kcal/mol), Leu207 (−2.673 kcal/mol), Ile202 (−2.841 kcal/mol), Met199 (−3.656 kcal/mol), Pro193 (−2.839 kcal/mol), Tyr158 (−2.71 kcal/mol), Ala157 (−2.525 kcal/mol), Pro156 (−2.425 kcal/mol), Met155 (−2.584 kcal/mol), Gly104 (−2.597 kcal/mol), Met103 (−2.43 kcal/mol) and Ser20 (−2.383 kcal/mol) residues, while the 5-nitro-2-(prop-2-yn-1-yloxy) benzylidene) section interacted similarly with Ile194 (−3.263 kcal/mol), Gly192 (−2.479 kcal/mol), Lys165 (−2.045 kcal/mol), Phe149 (−3.636 kcal/mol), Asp148 (−2.193 kcal/mol), Met147 (−2.333 kcal/mol), and Ser94 (−2.725 kcal/mol) residues. Furthermore, the isonicotinohydrazide component of the molecule also has displayed significant van der Waals interactions with Ala198 (−2.449 kcal/mol), Thr196 (−2.343 kcal/mol), Ala191 (−2.561 kcal/mol), Met161 (−2.096 kcal/mol), Met98 (−2.445 kcal/mol), Phe97 (−3.435 kcal/mol), Gly96 (−2.898 kcal/mol), Ile21 (−2.044 kcal/mol) and Ile16 (−2.271 kcal/mol) residues. The enhanced binding affinity of **5i** has been also attributed to very significant coulombic (electrostatic) interactions observed with Asp261 (−2.693 kcal/mol), Glu220 (−2.585 kcal/mol), Glu219 (−3.241 kcal/mol), Gln214 (−2.464 kcal/mol), Glu210 (−2.278 kcal/mol), Glu209 (−2.223 kcal/mol), Met199 (−2.47 kcal/mol), Thr196 (−2.847 kcal/mol), Arg195 (−2.393 kcal/mol), Ile194 (−2.455 kcal/mol), Lys165 (−3.51 kcal/mol), Pro156 (−2.228 kcal/mol), Asp150 (−2.867 kcal/mol), Asp148 (−2.427 kcal/mol), Met147 (−2.443 kcal/mol), Gly96 (−2.841 kcal/mol) and Ser20 (−2.361 kcal/mol) residues. While these non-bonded interactions i.e. steric and electrostatic with active site residues of InhA were the major driving force for the mechanical interlocking of **5i**, the higher binding affinity is also complemented by a very close hydrogen bonding interactions observed firstly with Ile194 through prop-2-yn-1-yloxy linker in the molecule and secondly with carbonyl (–C═O) function through the Thr196 residue having bond distances of 2.15 Å and 2.02 Å, respectively. Furthermore, the compound **5i** was seen to be anchored to InhA through two pi-pi(π-π) stacking interactions as well, firstly with Tyr158 (2.111 Å) and second observed through Phe149 (2.113 Å). Such type of hydrogen bonding and pi-pi stacking interactions serve as an anchor to direct the orientation of inhibitor into the 3D

Table 4

Per-residue interaction analysis data for isoniazid embedded triazole derivatives (**5b, 5d, 5f, 5i, 5j, 5m, 5n, 5o** and **5p**) with mycobacterial enoyl ACP reductase (InhA).

Entry & MIC (μg/mL)	Glide Score	Glide Interaction Energy (kcal/mol)	Per-Residues Interactions			
			Van der Waals (kcal/mol)	Coulombic (kcal/mol)	H-bonding (Å)	Pi-Pi Stacking (Å)
5b (0.78)	−8.217	−50.551	Leu218 (−2.342), Leu217 (−2.205), Ile215 (−3.224), Gln214(−2.334), Leu207 (−2.171), Ile202 (−2.326), Met199 (−3.256), Ala198 (−3.314), Thr196 (−2.227), Ile194 (−3.113), Pro193 (−2.249), Gly192 (−2.301), Ala191 (−2.418), Lys165 (−2.118), Met161 (−2.002), Tyr158 (−3.198), Ala157 (−2.361), Pro156 (−2.229), Met155 (−2.471), Phe149(−3.195), Asp148 (−2.124), Met147 (−2.222), Gly104 (−2.144), Met103 (−2.254), Met98 (−2.245), Phe97 (−3.235), Gly96 (−2.298), Ser94 (−2.225), Ile21 (−2.125), Ser20 (−2.113), Ile16 (−2.080)	Asp261 (−2.463), Glu220 (−2.275), Glu219 (−2.932), Gln214 (−2.261), Glu210 (−2.277), Glu209 (−2.351), Met199 (−2.360), Thr196 (−2.447), Arg195 (−2.253), Ile194 (−2.415), Lys165 (−2.342), Pro156 (−2.118), Asp150 (−2.167), Asp148 (−2.127), Met147 (−2.103), Gly96 (−2.184), Ser20 (−2.361)	Thr196 (2.17)	Phe149 (2.143)
5d (0.78)	−8.372	−51.71	Leu218 (−2.448), Leu217 (−2.476), Ile215 (−3.348), Gln214 (−2.626), Leu207 (−2.472), Ile202 (−2.619), Met199 (−3.443), Ala198 (−3.114), Thr196 (−2.233), Ile194 (−3.151), Pro193 (−2.557), Gly192 (−2.472), Ala191 (−2.523), Lys165 (−2.039), Met161 (−2.011), Tyr158 (−3.171), Ala157 (−2.462), Pro156 (−2.215), Met155 (−2.513), Phe149 (−3.499), Asp148 (−2.135), Met147 (−2.278), Gly104 (−2.195), Met103 (−2.391), Met98 (−2.342), Phe97 (−3.320), Gly96 (−2.554), Ser94 (−2.438), Ile21 (−2.023), Ser20 (−2.081), Ile16 (−2.211)	Asp261 (−2.553), Glu220 (−2.382), Glu219 (−3.041), Gln214 (−2.352), Glu210 (−2.458), Glu209 (−2.447), Met199 (−2.339), Thr196 (−2.556), Arg195 (−2.277), Ile194 (−2.426), Lys165 (−3.444), Pro156 (−2.208), Asp150 (−2.333), Asp148 (−2.193), Met147 (−2.122), Gly96 (−2.484), Ser20 (−2.636)	Ile194 (2.16), Thr196 (2.27), Glu104 (2.68), Ser94 (2.75)	Phe149 (2.23)
5f (1.56)	−7.836	−48.322	Leu218 (−2.134), Leu217 (−1.976), Ile215 (−2.067), Gln214 (−1.926), Leu207 (−1.773), Ile202 (−1.619), Met199 (−2.156), Ala198 (−2.114), Thr196 (−2.135), Ile194 (−2.112), Pro193 (−2.106), Gly192 (−1.727), Ala191 (−2.317), Lys165 (−2.043), Met161 (−1.607), Tyr158 (−1.736), Ala157 (−1.457), Pro156 (−1.525), Met155 (−1.678), Phe149 (−2.144), Asp148 (−2.011), Met147 (−2.111), Gly104 (−1.597), Met103 (−1.238), Met98 (−2.014), Phe97 (−1.435), Gly96 (−1.891), Ser94 (−1.725), Ile21 (−1.845), Ser20 (−2.088), Ile16 (−1.821)	Asp261 (−1.693), Glu220 (−2.041), Glu219 (−1.585), Gln214 (−1.564), Glu210 (−1.778), Glu209 (−1.791), Met199 (−1.999), Thr196 (−1.847), Arg195 (−1.893), Ile194 (−2.415), Lys165 (−1.641), Pro156 (−1.758), Asp150 (−1.666), Asp148 (−1.027), Met147 (−1.223), Gly96 (−1.442), Ser20 (−1.361)	Ile194	Tyr158 (2.589), Phe149 (2.518)
5i (0.78)	−8.395	−52.373	Leu218 (−2.599), Leu217 (−2.576), Ile215 (−3.547), Gln214 (−2.823), Leu207 (−2.673), Ile202 (−2.841), Met199 (−3.656), Ala198 (−2.449), Thr196 (−2.343), Ile194 (−3.263), Pro193 (−2.839), Gly192 (−2.479), Ala191 (−2.561), Lys165 (−2.045), Met161 (−2.096), Tyr158 (−2.71), Ala157 (−2.525), Pro156 (−2.425), Met155 (−2.584), Phe149 (−3.636), Asp148 (−2.193), Met147 (−2.333), Gly104 (−2.597), Met103 (−2.43), Met98 (−2.445), Phe97 (−3.435), Gly96 (−2.898), Ser94 (−2.725), Ile21 (−2.044), Ser20 (−2.383), Ile16 (−2.271)	Asp261 (−2.693), Glu220 (−2.585), Glu219 (−3.241), Gln214 (−2.464), Glu210 (−2.278), Glu209 (−2.223), Met199 (−2.47), Thr196 (−2.847), Arg195 (−2.393), Ile194 (−2.455), Lys165 (−3.51), Pro156 (−2.228), Asp150 (−2.867), Asp148 (−2.427), Met147 (−2.443), Gly96 (−2.841), Ser20 (−2.361)	Ile194 (2.15), Thr196 (2.02)	Tyr158 (2.111), Phe149 (2.113)
5j (1.56)	−7.925	−49.524	Leu218 (−2.112), Leu217 (−1.996), Ile215 (−2.043), Gln214 (−1.986), Leu207 (−1.893), Ile202 (−1.763), Met199 (−2.341), Ala198 (−2.313), Thr196 (−2.119), Ile194 (−2.046), Pro193 (−2.115), Gly192 (−1.880), Ala191 (−2.636), Lys165 (−1.943), Met161 (−1.867), Tyr158 (−1.973), Ala157 (−1.949), Pro156 (−1.925), Met155 (−1.973), Phe149 (−1.988), Asp148 (−2.087), Met147 (−2.054), Gly104 (−1.997), Met103 (−1.896), Met98 (−2.041), Phe97 (−2.543), Gly96 (−1.896), Ser94 (−1.626), Ile21(−1.975), Ser20 (−1.883), Ile16 (−1.991)	Asp261 (−1.893), Glu220 (−1.943), Glu219 (−2.343), Gln214 (−1.864), Glu210 (−1.843), Glu209 (−1.891), Met199 (−2.142), Thr196 (−1.829), Arg195 (−1.996), Ile194 (−2.051), Lys165 (−1.849), Pro156 (−1.608), Asp150 (−1.867), Asp148 (−1.031), Met147 (−1.443), Gly96 (−1.841), Ser20 (−1.561)	Ile194 (2.33)	Tyr158 (2.176), Phe149 (2.343)

Table 4 (*continued*)

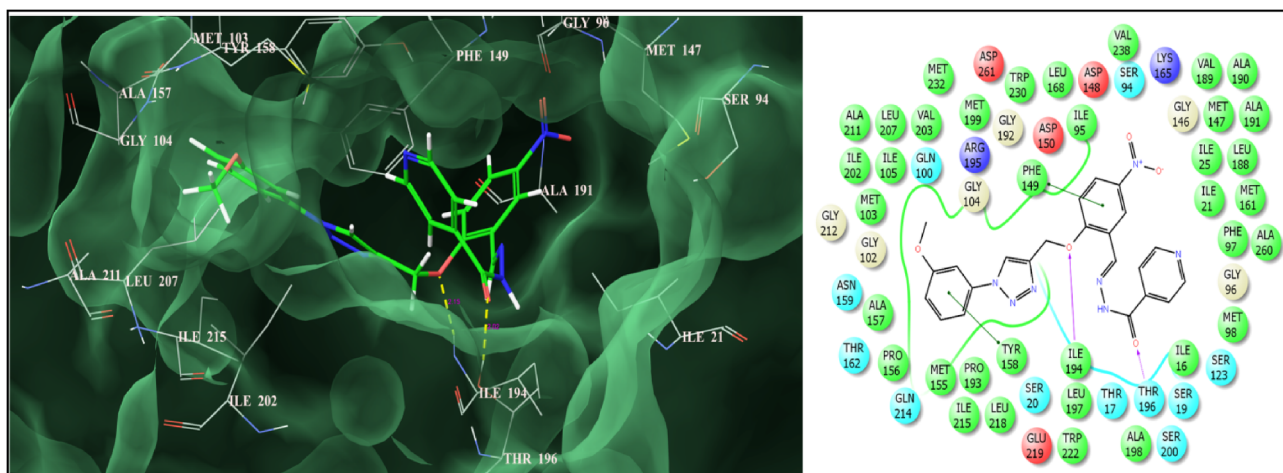| Entry & MIC (μg/mL)	Glide Score	Glide Interaction Energy (kcal/mol)	Per-Residues Interactions		H-bonding (Å)	Pi-Pi Stacking (Å)
			Van der Waals (kcal/mol)	Coulombic (kcal/mol)		
5m (0.78)	−8.225	−51.704	Leu218 (−2.241), Leu217 (−2.116), Ile215 (−3.154), Gln214 (−2.192), Leu207 (−2.073), Ile202 (−2.248), Met199 (−2.973), Ala198 (−2.925), Thr196 (−2.167), Ile194 (−3.207), Pro193 (−2.339), Gly192 (−2.216), Ala191 (−2.441), Lys165 (−2.113), Met161 (−2.095), Tyr158 (−2.949), Ala157 (−2.367), Pro156 (−2.235), Met155 (−2.404), Phe149 (−2.919), Asp148 (−2.087), Met147 (−2.215), Gly104 (−2.112), Met103 (−2.145), Met98 (−2.014), Phe97 (−3.225), Gly96 (−2.198), Ser94 (−2.232), Ile21 (−2.214), Ser20 (−2.083), Ile16 (−2.121)	Asp261 (−2.169), Glu220 (−2.134), Glu219 (−2.274), Gln214 (−1.216), Glu210 (−2.243), Glu209 (−2.191), Met199 (−2.247), Thr196 (−2.534), Arg195 (−2.193), Ile194 (−2.234), Lys165 (−2.489), Pro156 (−2.308), Asp150 (−2.261), Asp148 (−2.023), Met147 (−2.001), Gly96 (−2.441), Ser20 (−2.238)	Ile194 (2.52), Thr196 (2.07)	Phe149 (2.286)
5n (3.125)	−7.129	−45.67	Leu218 (−1.952), Leu217 (−1.706), Ile215 (−2.021), Gln214 (−1.192), Leu207 (−1.071), Ile202 (−1.486), Met199 (−1.887), Ala198 (−2.114), Thr196 (−2.131), Ile194 (−1.936), Pro193 (−1.898), Gly192 (−1.721), Ala191 (−2.302), Lys165 (−2.141), Met161 (−1.067), Tyr158 (−1.276), Ala157 (−1.162), Pro156 (−1.125), Met155 (−1.271), Phe149 (−1.206), Asp148 (−2.009), Met147 (−2.111), Gly104 (−1.197), Met103 (−1.135), Met98 (−2.011), Phe97 (−1.413), Gly96 (−1.189), Ser94 (−1.241), Ile21 (−1.291), Ser20 (−1.083), Ile16 (−1.211)	Asp261 (−1.564), Glu220 (−1.413), Glu219 (−1.101), Gln214 (−1.143), Glu210 (−1.324), Glu209 (−1.230), Met199 (−1.342), Thr196 (−1.590), Arg195 (−1.165), Ile194 (−2.039), Lys165 (−1.675), Pro156 (−1.208), Asp150 (−1.186), Asp148 (−1.111), Met147 (−1.003), Gly96 (−1.341), Ser20 (−1.131)	Ile194 (2.30)	Tyr158 (2.373), Phe149 (2.424)
5o (0.78)	−8.126	−50.349	Leu218 (−2.522), Leu217 (−2.207), Ile215 (−3.025), Gln214 (−2.128), Leu207 (−2.423), Ile202 (−2.146), Met199 (−3.053), Ala198 (−2.314), Thr196 (−2.235), Ile194 (−2.486), Pro193 (−2.265), Gly192 (−2.211), Ala191 (−2.388), Lys165 (−1.999), Met161 (−2.177), Tyr158 (−3.225), Ala157 (−3.062), Pro156 (−2.612), Met155 (−2.332), Phe149 (−2.245), Asp148 (−2.075), Met147 (−2.133), Gly104 (−2.119), Met103 (−2.143), Met98 (−2.020), Phe97 (−3.113), Gly96 (−2.143), Ser94 (−1.725), Ile21 (−2.421), Ser20 (−2.003), Ile16 (−2.023)	Asp261 (−2.233), Glu220 (−2.313), Glu219 (−3.012), Gln214 (−1.964), Glu210 (−2.488), Glu209 (−1.291), Met199 (−2.231), Thr196 (−2.147), Arg195 (−1.144), Ile194 (−2.455), Lys165 (−2.675), Pro156 (−1.605), Asp150 (−2.186), Asp148 (−2.126), Met147 (−2.113), Gly96 (−2.184), Ser20 (−2.236)	Tyr158 (2.30), Lys165 (2.44)	Phe149 (2.396)
5p (0.78)	−8.056	−50.259	Leu218 (−2.455), Leu217 (−2.736), Ile215 (−2.927), Gln214 (−2.669), Leu207 (−2.679), Ile202 (−2.486), Met199 (−2.967), Ala198 (−3.364), Thr196 (−2.632), Ile194 (−2.646), Pro193 (−2.439), Gly192 (−2.301), Ala191 (−2.234), Lys165 (−1.924), Met161 (−2.154), Tyr158 (−2.377), Ala157 (−2.285), Pro156 (−2.389), Met155 (−2.271), Phe149 (−2.168), Asp148 (−2.228), Met147 (−2.136), Gly104 (−2.137), Met103 (−2.106), Met98 (−2.172), Phe97 (−3.435), Gly96 (−2.391), Ser94 (−1.698), Ile21 (−2.293), Ser20 (−1.982), Ile16 (−1.992)	Asp261 (−2.221), Glu220 (−2.165), Glu219 (−2.935), Gln214 (−1.872), Glu210 (−2.274), Glu209 (−1.929), Met199 (−2.210), Thr196 (−2.129), Arg195 (−1.192), Ile194 (−2.143), Lys165 (−2.006), Pro156 (−1.518), Asp150 (−2.280), Asp148 (−1.027), Met147 (−1.988), Gly96 (−1.849), Ser20 (−1.966)	Lys165 (2.24), Gly96 (2.44)	Tyr158 (2.572)

Fig. 2. Binding mode of **5i** into the active site of mycobacterial enoyl ACP reductase (InhA). (On the right side: green lines indicate π-π stacking interactions, while the pink lines signify the hydrogen bonding interactions).

space of enzyme's active site and further facilitate the non-bonded interactions as well contributing to the stability of the enzyme-inhibitor complex. The other active molecules **5b, 5d, 5f, 5j, 5m, 5n, 5o** and **5p** (Figs. S1–S8) were also observed to be deeply embedded in the active site of InhA engaging in a network of bonded and non-bonded interactions. Overall, the binding affinity data along with the per-residue ligand interaction analysis suggests that a balanced network of non-bonded interactions (steric and electrostatic) complemented by hydrogen bonding and pi-pi stacking interactions contribute to the anchoring of these molecules to mycobacterial InhA. The quantitative insights derived herein are now being fruitfully utilized to carry out site specific mutation around the core nucleus to generate tighter binding and potent mycobacterial InhA inhibitors.

In conclusion, a series of novel isoniazid embedded triazole derivatives (**5a-p**) have been synthesized *via* click reaction in good to excellent yields. The newly synthesized compounds were evaluated for their *in vitro* antimycobacterial and antimicrobial activities. We have identified six compounds as potent antitubercular agents (MIC value 0.78 μg/mL) against *M. tuberculosis* H37Rv (*Mtb*). However, the three compounds have exhibited moderate antitubercular activity in the range of MIC value 1.56–3.12 μg/mL. These compounds have displayed low cytotoxicity profile by MTT assay against RAW 264.7 cell line. Among the compounds screened for their *in vitro* antimicrobial activities, five compound have shown good activities against both antibacterial and antifungal pathogens. Furthermore, in silico binding affinity data against mycobacterial InhA could provide a valuable insight into the plausible mechanism of antitubercular action for these molecules. The promising results obtained from this study qualifies these new isoniazid embedded triazole derivatives as a pertinent starting point for structure-based optimization as InhA specific antitubercular candidates through iterative design and synthesis approach. The new entities with dual antitubercular and antimicrobial properties are desperately needed, we believe that the analogues reported in this work will help global efforts for identification of potential lead molecules for further development.

Declaration of Competing Interest

The authors declare that they have no known competing financial interests or personal relationships that could have appeared to influence the work reported in this paper.

Acknowledgments

Authors are thankful to Birla Institute of Technology and Science-

Appendix A. Supplementary data

Supplementary material to this article containing ^{1}H NMR, ^{13}C NMR and HRMS spectrums of new compounds are available for the authorized users. Supplementary data to this article can be found online at https://doi.org/10.1016/j.bmcl.2020.127434.

References

1. Ang MLT, Zainul Rahim SZ, de Sessions PF, et al. *Front Microbiol.* 2017;8:710.
2. World Health Organization (WHO), WHO Global Tuberculosis Report 2019, WHO, Geneve, Switzerland, 2019. http://www.who.int/tb/publications/global_report/en/.
3. Bahuguna A, Rawat DS. *Med Res Rev.* 2020;40:693.
4. Garrido-Cardenas JA, de Lamo-Sevilla C, Cabezas-Fernández MT, Manzano-Agugliaro F, Martínez-Lirola M. *Tuberculosis.* 2020;121:101917.
5. Koul A, Arnoult E, Lounis N, Guillemont J, Andries K. *Nature.* 2011;469:483.
6. Singh V, Mizrahi V. *Drug Discov Today.* 2016;22:503.
7. Eldehna WM, Fares M, Abdel-Aziz MM, Abdel-Aziz HA. *Molecules.* 2015;20:8800.
8. Denholm JT, McBryde ES, Eisen DP, Penington JS, Chen C, Street AC. *Drug Healthc Patient Saf.* 2014;6:145.
9. Beena, Rawat DS. *Med Res Rev.* 2013;33:693.
10. http://www.ctri.nic.in/Clinicaltrials/pmaindet2.php?trialid=922.
11. Hu Y-Q, Zhang S, Zhao F, et al. *Eur J Med Chem.* 2017;133:255.
12. Kumar D, Khare G, Beena, Kidwai S, Tyagi AK, Singh R, Rawat DS. *Med. Chem. Commun.* 2015;6:131.
13. Kumar D, Beena, Khare G, Kidwai S, Tyagi AK, Singh R, Rawat DS. *Eur J Med Chem.* 2014;81:301.
14. Judge V, Narasimhan B, Ahuja M, et al. *Med Chem Res.* 1935;2012:21.
15. Zhang S, Xu Z, Gao C, et al. *Eur J Med Chem.* 2017;138:501.
16. Boechat N, Ferreira VF, Ferreira SB, et al. *J Med Chem.* 2011;54:5988.
17. Nalla V, Shaikh A, Bapat S, et al. *Soc. Open sci.* 2018;5:171750.
18. Sajja Y, Vanguru S, Vulupala HR, et al. *Bioorg Med Chem Lett.* 2017;27:5119.
19. Xia X, Zhang Q, Zhao L, Hu Y. *Eur J Med Chem.* 2017;138:66.
20. Smit FJ, Seldon R, Aucamp J, Jordaan A, Warner DF, N'Da DD. *Med Chem Res.* 2019;28:2279.
21. Rizvi F, Khan M, Jabeen A, Siddiqui H, Choudhary MI. *Sci Rep.* 2019;9:6738.
22. Phatak PS, Bakale RD, Dhumal ST, et al. *Synth Commun.* 2017;2019:49.
23. Skripconoka V, Danilovits M, Pehme L, et al. *Eur Respir J.* 2013;41:1393.
24. Sasaki H, Haraguchi Y, Itotani M, et al. *J Med Chem.* 2006;49:7854.
25. Makarov V, Lechartier B, Zhang M, et al. *EMBO Mol Med.* 2014;6:372.
26. Kumar D, Negi B, Rawat DS. *Future Med Chem.* 1981;2015:14.
27. Oliveira PFM, Guidetti B, Chamayou A, et al. *Molecules.* 2017;22:1457.
28. Shanmugavelan P, Nagarajan S, Sathishkumar M, Ponnuswamy A, Yogeeswari P, Sriram D. *Bioorg Med Chem Lett.* 2011;21:7273.
29. Muluk MB, Dhumal ST, Phatak PS, et al. *J Heterocycl Chem.* 2019;56:2411.
30. Muluk MB, Dhumal ST, Rehman NNMA, Dixit PP, Kharat KR, Haval KP. *ChemistrySelect.* 2019;4:8993.
31. Muluk MB, Phatak PS, Pawar SB, et al. *J Chin Chem Soc.* 2019;66:1507.
32. Collins LA, Franzblau SG. *Antimicrob Agents Chemother.* 1997;41:1004.

33. Krishna VS, Zheng S, Rekha EM, Guddat LW, Sriram D. *J Comput Aided Mol Des.* 2019;33:357.
34. Van Meerloo J, Kaspers GJ, Cloos J. *Methods Mol Biol.* 2011;731:237.
35. Phatak PS, Sathe BP, Dhumal ST, et al. *J Heterocycl Chem.* 1928;2019:56.
36. Khare SP, Deshmukh TR, Sangshetti JN, et al. *ChemistrySelect.* 2018;3:13113.
37. Shaikh MH, Subhedar DD, Arkile M, et al. *Bioorg Med Chem Lett.* 2016;26:561.
38. Friesner RA, Banks JL, Murphy RB, et al. *J Med Chem.* 2004;47:1739.
39. Banerjee A, Dubnau E, Quemard A, et al. *Science.* 1994;263:227.
40. Halgren TA, Murphy RB, Friesner RA, et al. *J Med Chem.* 2004;47:1750.
41. Molecular docking study: The Glide (Grid-Based Ligand Docking With Energetics) program (Schrödinger, LLC, New York, NY, 2018) was used to perform the molecular docking study for which the 3D crystal structure of mycobacterial enoyl-ACP reductase (InhA) complexed with its inhibitor (PDB code: 4TZK) was retrieved from the RCSB's Protein Data Bank (http://www.rcsb.org/pdb/) and refined using the Protein Preparation Wizard to correct the experimental errors which involve elimination of all crystallographically observed water molecules (since they are not known to be conserved in the ligand interaction), adding the missing hydrogen atoms and side chains, assignment of all atom force field (OPSL-2005) charges and atom types, creating the disulfide bonds, identification of atom/residue overlaps and finally energy minimization of the cleaned structure until the average RMSD of nonhydrogen atoms converged to 0.3 Å. Next, the shape and properties of the active site of the enzyme for docking was defined using the receptor grid generation panel to include residues within a 10.0 Å radius of the crystallized ligand for which a grid box of 10X10X10Å dimensions around the centroid of the native ligand was generated. The 2D structures of the ligands to be docked were sketched with the build panel in Maestro and converted using the ligand preparation panel to energy minimized 3D structures. This ligand optimization procedure involves assignment of correct protonation states and atom types to the molecule, ascribing partial atomic charges (OPLS-2005 force field) and then final energy minimization (until their average RMSD reached 0.001Å) to generate single low energy 3D structure for docking. With this setup, flexible docking was executed with extra precision (i.e., with GlideXP) scoring function to identify the modes of binding for these bioactive molecule and gauze their binding affinities towards InhA. The docking poses generated as output file analyzed for the most significant thermodynamic interactions with the active site residues through the Pose Viewer utility of Maestro.
42. Procedure for the synthesis of 5-nitro-2-(prop-2-yn-1-yloxy)benzaldehyde (2): A mixture of 2-hydroxy-5-nitrobenzaldehyde (1) (1 mmol), propargyl bromide (80 wt% in toluene) (1.5 mmol) and K2CO3 (1.5 mmol) was stirred in DMF at room temperature for 6h. The progress of the reaction was monitored by TLC. After completion of reaction, the reaction mixture was poured on crushed ice. The solid obtained was filtered, washed with water and crystallized from ethanol. Yield: 90%; M. P.: 90-92°C.
43. Procedure for the synthesis of (E)-N'-(5-nitro-2-(prop-2-yn-1-yloxy)benzylidene)isonicotinohydrazide (3): A mixture of 5-nitro-2-(prop-2-yn-1-yloxy)benzaldehyde (2) (1 mmol) and isonicotinohydrazide (1 mmol) was dissolved in diisopropylethylammonium aceate (DIPEAc) (10 ml) and stirred at room temperature for 1h. Then, the reaction mixture was poured on cold water. The solid obtained was filtered and washed with cold water. The products obtained were crystallized from ethanol. (E)-N'-(5-Nitro-2-(prop-2-yn-1-yloxy) benzylidene)isonicotinohydrazide (3): Yield: 92%; M. P. : 205-207°C; 1H NMR (400 MHz, DMSO-d6) δ = 3.14 (t, J = 4 Hz, 1H), 4.93 (d, J = 4 Hz, 2H), 7.21 (d, J = 8 Hz, 1H), 7.80-7.84 (m, 3H), 8.21 (dd, J = 4 & 8 Hz, 1H), 8.70 (bs, 1H), 8.77-8.78 (m, 2H), 12.17 (s, 1H); 13C NMR (100 MHz, CDCl3 + DMSO-d6) δ = 56.76, 76.75, 78.04, 112.78, 121.44, 121.47, 123.41, 126.09, 139.85, 141.49, 142.17, 149.82, 159.74, 161.71.
44. General procedure for the synthesis of (E)-N'-(5-nitro-2-((1-phenyl-1H-1,2,3-triazol-4-yl)methoxy)benzylidene)isonicotinohydrazide derivatives (5a-p): The mixture of (E)-N'-(5-nitro-2-(prop-2-yn-1-yloxy)benzylidene)isonicotinohydrazide (3) (1 mmol) and substituted azidobenzenes (4a-p) (1 mmol) were stirred in presence of CuSO4.5H2O (20 mol%) and sodium ascorbate (20 mol%) in DMF at room temperature. The progress of the reactions was monitored by TLC. After completion of reactions (6-8h), the reaction mixtures were poured in ice cold water. The products obtained were filtered, washed with water and crystallized from ethanol. (E)-N'-(2-((1-(4-Chlorophenyl)-1H-1,2,3-triazol-4-yl)methoxy)-5-nitrobenzylidene) isonicotinohydrazide (5a): Yield: 83%; M. P.: 238-240°C; 1H NMR (400 MHz, DMSO-d6) δ = 5.42 (s, 2H), 7.35-7.38 (m, 1H), 7.47-7.50 (m, 2H), 7.72-7.73 (m, 3H), 7.81-7.84 (m, 3H), 8.24 (dd, J = 4 & 8 Hz, 1H), 8.72-8.79 (m, 3H), 12.08 (s, 1H). (E)-N'-(5-Nitro-2-((1-phenyl-1H-1,2,3-triazol-4-yl) methoxy)benzylidene)isonicotino hydrazide (5b): Yield: 85%; M. P.: 210-212°C; 1H NMR (400 MHz, DMSO-d6) δ = 5.45 (s, 2H), 7.41-7.54 (m, 3H), 7.82-7.85 (m, 2H), 7.88-7.94 (m, 5H), 8.26 (dd, J = 4 & 8 Hz, 1H), 8.76-8.81 (m, 3H), 12.15 (s, 1H). (E)-N'-(2-((1-(4-Bromophenyl)-1H-1,2,3-triazol-4-yl)methoxy)-5-nitrobenzylidene)isonicotinohydrazide (5c): Yield: 82%; M. P.: 225-227°C; 1H NMR (400 MHz, DMSO-d6) δ = 5.41 (s, 2H), 7.33-7.44 (m, 1H), 7.63-7.68 (m, 2H), 7.74-7.79 (m, 3H), 7.81-7.85 (m, 3H), 8.20-8.27 (m, 1H), 8.73-8.81 (m, 3H), 12.08 (s, 1H). (E)-N'-(5-Nitro-2-((1-(3-nitrophenyl)-1H-1,2,3-triazol-4-yl)methoxy)benzylidene) isonicotinohydrazide (5d): Yield: 92%; M. P.: 254-256°C; 1H NMR (400 MHz, DMSO-d6) δ = 5.49 (s, 2H), 7.46 (d, J = 8 Hz, 1H), 7.79-7.84 (m, 2H), 7.85 (m, 3H), 8.25 (d, J = 8 Hz, 2H), 8.36 (d, J = 8 Hz, 1H), 8.75-8.78 (m, 3H), 9.14 (s, 1H), 12.16 (s, 1H). (E)-N'-(2-((1-(4-Methoxyphenyl)-1H-1,2,3-triazol-4-yl)methoxy)-5-nitrobenzylidene) isonicotinohydrazide (5e): Yield: 84%; M. P.: 242-244°C; 1H NMR (400 MHz, DMSO-d6) δ = 3.85 (s, 3H), 5.41 (s, 2H), 7.06 (t, J = 8 Hz, 1H), 7.12 (d, J = 8 Hz, 1H), 7.362-7.43 (m, 2H), 7.64-7.77 (m, 5H), 8.23 (dd, J = 4 & 8 Hz, 1H), 8.41 (s, 1H), 8.74 (s, 1H), 8.81 (d, J = 2 Hz, 1H), 12.11 (s, 1H); 13C NMR (100 MHz, CDCl3 + DMSO-d6) δ = 55.10, 61.63, 111.61, 112.01, 120.14, 121.25, 122.69, 124.19, 124.63, 125.85, 129.70, 131.90, 139.36, 140.41, 140.76, 142.14, 150.08, 160.15, 161.43; HRMS (ESI)+ calcd. for C23H19N7O5 [M

+H]+: 474.1481 and found 474.1525. (E)-N'-(2-((1-(2-Chlorophenyl)-1H-1,2,3-triazol-4-yl)methoxy)-5-nitrobenzylidene) isonicotinohydrazide (5f): Yield: 82%; M. P.: 216-218°C; 1H NMR (400 MHz, DMSO-d6) δ = 5.40 (s, 2H), 7.02-7.10 (m, 1H), 7.25-7.35 (m, 1H), 7.39-7.48 (m, 2H), 7.541-7.58 (m, 2H), 7.62-7.67 (m, 2H), 7.77 (bs, 1H), 8.21 (dd, J = 4 & 8 Hz, 1H), 8.31-8.41 (m, 1H), 8.74-8.76 (m, 1H), 8.80-8.85 (m, 1H), 12.05 (s, 1H); 13C NMR (100 MHz, CDCl3 + DMSO-d6) δ = 61.48, 112.12, 120.04, 122.58, 124.11, 125.49, 125.79, 126.85, 127.19, 127.50, 129.68, 129.85, 130.35, 133.36, 140.70, 140.84, 142.02, 150.02, 159.98, 161.33 HRMS (ESI)+ calcd. for C22H16ClN7O4 [M+H]+: 478.0986 and found 478.1023. (E)-N'-(2-((1-(2-Methoxyphenyl)-1H-1,2,3-triazol-4-yl)methoxy)-5-nitrobenzylidene) isonicotinohydrazide (5g): Yield: 86%; M. P.: 126-128°C; 1H NMR (400 MHz, DMSO-d6) δ = 3.85 (s, 3H), 5.41 (s, 2H), 7.05-7.13 (m, 2H), 7.34-7.44 (m, 2H), 7.63-7.66 (m, 1H), 7.68-7.70 (m, 3H), 7.80 (bs, 1H), 8.24 (dd, J = 4 & 8 Hz, 1H), 8.40 (d, J = 8 Hz, 1H), 8.73 (d, J = 4 Hz, 1H), 8.80-8.83 (m, 1H), 12.11 (s, 1H); 13C NMR (100 MHz, CDCl3 + DMSO-d6) δ = 55.00, 60.27, 111.54, 114.78, 120.02, 121.07, 121.54, 122.58, 122.63, 123.35, 123.75, 124.04, 125.39, 129.59, 136.83, 139.35, 141.95, 144.90, 150.00, 160.05, 161.30. (E)-N'-(2-((1-(3-Chlorophenyl)-1H-1,2,3-triazol-4-yl)methoxy)-5-nitrobenzylidene) isonicotinohydrazide (5h): Yield: 84%; M. P.: 220-222°C; 1H NMR (400 MHz, DMSO-d6) δ = 5.43 (s, 2H), 7.35-7.40 (m, 2H), 7.46-7.50 (m, 1H), 7.73 (bs, 3H), 7.79-7.84 (m, 2H), 7.93 (bs, 1H), 8.24 (d, J = 8 Hz, 1H), 8.74-8.81 (m, 3H), 12.08 (s, 1H); 13C NMR (100 MHz, CDCl3 + DMSO-d6) δ = 61.81, 112.07, 114.98, 117.55, 119.39, 121.79, 122.71, 125.97, 127.90, 130.26, 134.19, 136.68, 140.85, 141.39, 142.28, 142.64, 148.83, 151.58, 160.06, 161.53. (E)-N'-(2-((1-(3-Methoxyphenyl)-1H-1,2,3-triazol-4-yl)methoxy)-5-nitrobenzylidene) isonicotinohydrazide (5i): Yield: 81%; M. P.: 232-234°C; 1H NMR (400 MHz, DMSO-d6) δ = 3.83 (s, 3H), 5.45 (s, 2H), 6.94-6.98 (m, 1H), 7.41-7.42 (m, 2H), 7.46-7.48 (m, 2H), 7.8 (bs, 3H), 7.95 (d, J = 4 Hz, 1H), 8.26 (dd, J = 4 & 8 Hz, 1H), 8.75 (s, 2H), 8.85 (s, 2H), 12.16 (s, 1H); 13C NMR (100 MHz, CDCl3 + DMSO-d6) δ = 54.24, 61.23, 104.63, 110.76, 111.84, 112.98, 119.88, 120.58, 121.71, 122.01, 125.53, 129.41, 134.42, 136.21, 140.20, 141.34, 141.43, 150.86, 158.98, 159.69. (E)-N'-(5-Nitro-2-((1-(o-tolyl)-1H-1,2,3-triazol-4-yl)methoxy)benzylidene) isonicotino hydrazide (5j): Yield: 83%; M. P.: 228-230°C; 1H NMR (400 MHz, DMSO-d6) δ = 2.16 (s, 3H), 5.44 (s, 2H), 7.30-7.40 (m, 4H), 7.66 (bs, 3H), 7.75 (d, J = 8 Hz, 2H), 7.22-7.25 (m, 1H), 8.67 (bs, 3H), 8.77 (s, 1H), 8.81 (d, J = 4 Hz, 1H), 12.07 (s, 1H); 13C NMR (100 MHz, CDCl3 + DMSO-d6) δ = 16.83, 61.68, 111.99, 120.66, 120.70, 121.22, 122.69, 124.81, 125.74, 125.91, 128.99, 130.51, 132.28, 135.09, 139.35, 140.72, 140.86, 142.05, 149.15, 159.98, 161.28; HRMS (ESI)+ calcd. for C23H19-N7O4 [M+H]+: 458.1581, and found 458.1581. (E)-N'-(2-((1-(2-Fluorophenyl)-1H-1,2,3-triazol-4-yl)methoxy)-5-nitrobenzylidene) isonicotinohydrazide (5k): Yield: 82%; M. P.: 220-222°C; 1H NMR (400 MHz, DMSO-d6) δ = 5.44 (s, 2H), 7.31-7.38 (m, 3H), 7.43-7.49 (m, 1H), 7.68 (d, J = 8 Hz, 1H), 7.75-7.90 (m, 3H), 8.22 (dd, J = 4 & 8 Hz, 1H), 8.46 (d, J = 4 Hz, 1H), 8.67 (bs, 1H), 8.73 (d, J = 8 Hz, 1H), 8.79-8.81 (m, 1H), 12.09 (s, 1H); 13C NMR (100 MHz, CDCl3 + DMSO-d6) δ = 61.40, 112.03, 116.05, 116.25, 121.26, 122.65, 124.42, 124.46, 124.76, 125.83, 129.98, 130.05, 140.74, 141.39, 142.12, 143.96, 149.14, 151.32, 160.01, 161.37. (E)-N'-(5-Nitro-2-((1-(m-tolyl)-1H-1,2,3-triazol-4-yl)methoxy)benzylidene) isonicotinohydrazide (5l): Yield: 86%; M. P.: 230-232°C; 1H NMR (400 MHz, DMSO-d6) δ = 2.38 (s, 3H), 5.41 (s, 2H), 7.21 (d, J = 8 Hz, 1H), 7.32-7.38 (m, 2H), 7.55 (d, J = 8 Hz, 1H), 7.59-7.64 (m, 3H), 7.76-7.78 (m, 2H), 8.21 (d, J = 8 Hz, 1H), 8.54 (d, J = 4 Hz, 1H), 8.75 (s, 1H), 8.80 (d, J = 4 Hz, 1H), 12.04 (s, 1H). (E)-N'-(2-((1-Mesityl-1H-1,2,3-triazol-4-yl)methoxy)-5-nitrobenzylidene)isonicotinohydrazide (5m): Yield: 80%; M. P.: 222-224°C; 1H NMR (400 MHz, DMSO-d6) δ = 1.87 (s, 6H), 2.29 (s, 3H), 5.46 (s, 2H), 6.93-6.98 (m, 2H), 7.34-7.37 (m, 1H), 7.69 (s, 1H), 7.73-7.77 (m, 2H), 8.06-8.08 (m, 1H), 8.21 (dd, J = 4 & 8 Hz, 1H), 8.68 (bs, 1H), 8.77-8.81 (m, 2H), 12.09 (s, 1H); 13C NMR (100 MHz, CDCl3 + DMSO-d6) δ = 16.50, 20.29, 62.18, 112.30, 121.74, 123.13, 125.14, 125.99, 128.32, 132.36, 134.00, 139.39, 139.73, 139.74, 141.08, 141.25, 142.56, 149.43, 160.22, 161.78 (E)-N'-(2-((1-(2,4-Dimethylphenyl)-1H-1,2,3-triazol-4-yl)methoxy)-5-nitrobenzylidene)isonicotinohydrazide (5n): Yield: 82%; M. P.: 248-250°C; 1H NMR (400 MHz, DMSO-d6) δ = 2.12 (s, 3H), 2.35 (s, 3H), 5.46 (s, 2H), 7.12 (d, J = 8 Hz, 1H), 7.17-7.22 (m, 2H), 7.45 (d, J = 8 Hz, 1H), 7.80 (bs, 1H), 7.47 (s, 3H), 8.25 (dd, J = 4 & 8 Hz, 1H), 8.34 (s, 1H), 8.74-8.79 (m, 2H), 12.15 (s, 1H); 13C NMR (100 MHz, CDCl3 + DMSO-d6) δ = 16.37, 19.65, 61.35, 112.06, 113.05, 120.64, 122.28, 124.34, 124.82, 125.52, 126.14, 130.67, 131.56, 132.41, 135.19, 138.56, 140.45, 141.68, 144.01, 148.12, 159.77, 160.94; HRMS (ESI)+ calcd. for C24H21N7O4 [M+H]+: 472.1689 and found 472.1721. (E)-N'-(2-((1-(2-Methyl-5-nitrophenyl)-1H-1,2,3-triazol-4-yl)methoxy)-5-nitro benzylidene)isonicotinohydrazide (5o): Yield: 90%; M. P.: 250-252°C; 1H NMR (400 MHz, DMSO-d6) δ = 2.33 (s, 3H), 5.45 (s, 2H), 7.33 (d, J = 8 Hz, 1H), 7.58-7.61 (m, 3H), 7.77 (bs, 1H), 7.79 (s, 1H), 8.21-8.25 (m, 3H), 8.48 (s, 1H), 8.77-8.78 (m, 2H), 12.02 (s, 1H); 13C NMR (100 MHz, CDCl3 + DMSO-d6) δ = 18.67, 62.75, 112.97, 121.20, 122.88, 123.79, 124.47, 126.04, 126.91, 132.88, 136.61, 140.41, -141.52, 141.90, 142.69, 143.04, 143.64, 146.41, 150.36, 161.01, 162.55; HRMS (ESI)+ calcd. for C23H18N8O6 [M+H]+: 503.1383 and found 503.1427. (E)-N'-(2-((1-(4-Ethylphenyl)-1H-1,2,3-triazol-4-yl)methoxy)-5-nitrobenzylidene) isonicotinohydrazide (5p): Yield: 84%; M. P.: 234-236°C; 1H NMR (400 MHz, DMSO-d6) δ = 1.20 (t, J = 8 Hz, 3H), 2.665 (q, J = 8 Hz, 2H), 5.40 (s, 2H), 7.30 (d, J = 8 Hz, 1H), 7.34 (s, 1H), 7.63 (s, 3H), 7.64 (d, J = 8 Hz, 1H), 7.76 (bs, 1H), 8.23 (dd, J = 4 & 8 Hz, 1H), 8.52 (s, 1H), 8.75 (s, 1H), 8.81 (d, J = 2 Hz, 1H), 12.04 (s, 1H); 13C NMR (100 MHz, CDCl3 + DMSO-d6) δ = 15.16, 26.63, 62.42, 113.29, 117.35, 120.02, 123.39, 126.38, 128.84, 134.59, 136.59, 138.12, 139.60, 141.54, 142.38, 145.08, 147.39, 149.88, 159.26, 163.31; HRMS (ESI)+ calcd. for C24H21N7O4 [M+H]+: 472.1689 and found 472.1735.